Ionics (2023) 29:4037–4054
https://doi.org/10.1007/s11581-023-05115-7

RESEARCH

Synthesis of biopolymer electrolyte using sodium alginate with ammonium perchlorate (NH_4ClO_4) for the application of electrochemical devices

Vanitha N[1,3] · Shanmugapriya C[1] · Selvasekarapandian S[2,3] · Muniraj Vignesh N[3,4] · Aafrin Hazaana S[3,5] · Meera Naachiyar R[3,5] · Kamatchi Devi S[1,3]

Received: 28 April 2023 / Revised: 10 June 2023 / Accepted: 6 July 2023 / Published online: 12 July 2023

Abstract
Biopolymer electrolyte based on sodium alginate (NaAlg) with various concentrations of NH_4ClO_4 has been prepared by solution casting technique using double distilled water as solvent. Influence of different concentrations of NH_4ClO_4 on the biopolymer NaAlg is systematically investigated by the different characterization techniques such as XRD, FTIR, DSC, TGA, electrical impedance spectroscopy analysis, transference number measurement, and LSV. XRD was used to investigate whether the prepared biopolymers were crystalline or amorphous. The formation of complexes between NaAlg and NH_4ClO_4 has been observed by FTIR. Using differential scanning calorimeter, glass transition temperature (T_g) is found for the prepared biopolymer electrolyte. The maximum ionic conductivity of 3.59×10^{-3} S cm^{-1} has been obtained for 30 M.wt% NaAlg:70 M.wt% NH_4ClO_4 biopolymer electrolyte using AC impedance analysis. Using DC Wagner's polarization technique, the ionic transference number has been determined. The highest conducting biopolymer electrolyte's electrochemical stability window was found by the LSV technique to be 2.71 V. The primary proton battery and proton exchange membrane (PEM) fuel cell have been constructed using highest ionic conducting biopolymer membrane (30 M.wt% NaAlg:70 M.wt% NH_4ClO_4), and the performance has been studied. The proton battery's open circuit voltage (V_{oc}) is 1.76 V, while the PEM fuel cell's open circuit voltage (V_{oc}) is 789 mV.

Keywords Sodium alginate · XRD · TGA · PEM fuel cell · LSV

✉ Selvasekarapandian S
sekarapandian@rediffmail.com

1 PG & Research Department of Physics, Sri Paramakalyani College, Alwarkurichi - 627412, Affiliated to Manonmaniam Sundaranar University, Abishekapatti, Tirunelveli 627012, Tamil Nadu, India

2 Bharathiar University, Coimbatore 641046, Tamil Nadu, India

3 Materials Research Center, Coimbatore 641045, Tamil Nadu, India

4 Research Centre of Physics, Mannar Thirumalai Naicker College (Affiliated With Madurai Kamaraj University), Madurai 625004, Tamil Nadu, India

5 Research Centre of Physics, Fatima College (Affiliated with Madurai Kamaraj University), Madurai 625018, Tamil Nadu, India

Introduction

In the development of science and technology, electrochemical device like battery plays a crucial role which is employed as a power source in a wide range of portable devices and electric vehicles [1]. In electrochemical devices, biopolymer electrolytes are frequently considered as alternatives to synthetic polymer electrolytes [2]. Solid biopolymeric electrolytes make a positive contribution to ionic conductivity, electrochemical stability, flexibility, and light weight [3–5]. Over the past decade, several biopolymers such as dextrin, starch, chitosan, pectin, carrageenan, agar, cellulose, and corn starch derivatives have been used to prepare environmentally sustainable electrolytes [6].

Sodium alginate (NaAlg) biopolymer is a type of polysaccharide derived from the cell of brown marine algae. It is made up of $1\rightarrow4$ linked β-D-guluronic (G), and α-L-mannuronic (M) molecule [7, 8]. Polymeric segment -M-G blocks are combined to form uronic acids (Fig. 1) [9].

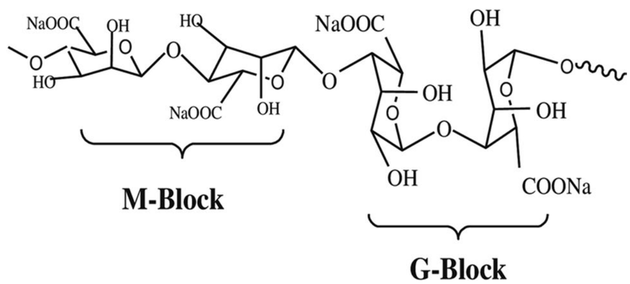

Fig. 1 Molecular structure of sodium alginate

Biopolymer NaAlg find its application in various fields such as food packaging [10], grafting copolymerization [11], emulsifiers, stabilizers [12], cosmetics [13], drug delivery [14, 15], medical applications [16], and textiles [17]. As of now, not many researches have been done using NaAlg as a electrolyte material. For a material to be used as an electrolyte, it should have a sufficient number of polar groups to which any salt cation can get attached. NaAlg has a large number of polar groups to which any salt's cation can be attached [18, 19]. Biopolymer NaAlg will not pollute the environment. In this paper, it has been used as an electrolyte material.

Few works have been done on the preparation of NaAlg-based biopolymer electrolyte with different salts. Jansi et al. have prepared PVA:NaAlg with NH_4Cl solid polymer electrolyte[20]. Iwaki et al. had prepared sodium alginate solid polymer electrolyte and reported a maximum conductivity value of 3.1×10^{-4} S cm^{-1} for the composition of 42.5Wt% of NaAlg:15 wt% $LiClO_4$:42.5Wt% glycerol [18]. Fuzlin et al. has reported ionic conductivity value of 5.32×10^{-5} S cm^{-1} for the composition of 1 g NaAlg with 20 wt% glycolic acid [5]. Ionic conductivity values of 2.0×10^{-3} S cm^{-1}, 2.29×10^{-3} S cm^{-1}, and 1.22×10^{-2} S cm^{-1} have been reported by Diana et al. for the composition of 30 wt% NaAlg:70 wt% NaI, 40 wt% NaAlg:60 wt% $NaClO_4$, and 30 wt% NaAlg:70 wt% NaSCN respectively [21–23]. Tamilisai et al. have reported ionic conductivity value of 4.58×10^{-3} S cm^{-1} for the composition of 40 M.wt% NaAlg:60 M.wt% $Mg(NO_3)_2.6H_2O$ [24].

Amorphous phase of the biopolymer is improved by the addition of salt, which perturbs the biopolymer network. Ammonium salts are considered as proton donor because one of proton of ammonium ion is loosely bound. Lattice energy of the ammonium salt is low which makes it highly soluble in water [25, 26].

Ionic conductivity values for many biopolymers with ammonium salts have been obtained from literature reviews. Selvalakshmi et al. measured conductivity values of 1.17×10^{-4} S cm^{-1} and 3.73×10^{-4} S cm^{-1} for 50 mol% agar agar:50 mol% NH_4I and 50 wt% agar agar:50 wt% NH_4Br respectively [27, 28]. Ionic conductivity value for 1 g of K-carrageenan–based NH_4SCN has been reported by Selvin et al. as 6.83×10^{-4} S cm^{-1} [25]. Shujahadeen et al. have reported the conductivity values of 3.07×10^{-8} S cm^{-1} and 8.57×10^{-4} S cm^{-1} for the composition of 40 wt% chitosan:30 wt% potato starch:30 wt% NH_4BF_4 and 1-g chitosan:40wt% NH_4SCN:40wt% glycerol respectively [29, 30]. Sohaimy et al. have reported the ionic conductivity values of 7.71×10^{-6} S cm^{-1} and 1.47×10^{-4} S cm^{-1} for 2-g carboxymethyl cellulose:7wt% $(NH_4)_2CO_3$ and 1-g carboxymethyl cellulose with 40wt% NH_4HCO_2 respectively [31, 32]. Ramli et al. have reported the ionic conductivity value of 1.16×10^{-4} S cm^{-1} for 2-g 2-hydroxyethyl cellulose with 36 wt% NH_4SCN [33]. Muthukrishnan et al. measured conductivity values of 4.5×10^{-3} S cm^{-1}, 2.74×10^{-4} S cm^{-1}, and 3.6×10^{-3} S cm^{-1} for 30 M.wt% pectin: 70 M.wt% NH_4I, 50 M.wt% pectin:50 M.wt%NH_4CO_2 and 50 M.wt% pectin:50 M.wt% NH_4HCO_2:0.4wt% ethylene carbonate respectively [34, 35]. Ionic conductivity value of 8.03×10^{-3} S cm^{-1} has been reported by Maheshwari et al. for the composition of 700-mg dextran:300-mg PVA:0.6 M.wt% NH_4SCN [36]. Meera Naachiyar et al. have reported ionic conductivity value of 5.62×10^{-3} S cm^{-1} for the composition of 1-g gellan gum:0.9wt% NH_4HCO_2 [37].

Vanitha et al. have investigated a proton battery based on biopolymer NaAlg with NH_4SCN and NaAlg with NH_4HCO_2 [26, 38]. Research work using NaAlg for proton battery is very limited. So an attempt is made to develop a NaAlg-based proton battery and single fuel cell.

In the present study, proton-conducting biopolymer electrolytes were prepared using NaAlg and NH_4ClO_4. The prepared samples are characterized by various techniques, namely X-ray diffraction (XRD), Fourier transform infrared spectroscopy (FTIR), differential scanning calorimetry (DSC), thermogravimetric analyzer (TGA), electrical impedance spectroscopy analysis, and linear sweep voltammetry (LSV). The transference number of the H + ion is calculated using Wagner's polarization techniques. Using the highest conducting biopolymer electrolyte, the primary proton battery and proton exchange membrane (PEM) fuel cell have been developed. The results are discussed and presented in this paper.

Materials and methods

Materials

Sodium alginate biopolymer (S D Fine-Chem limited molecular weight 216.12 g/mol) as a host polymer. Ammonium perchlorate (Merck Specialities Private Limited: MW 117.49 g/mol) is the salt. The solvent is double-distilled (DD) water.

Preparation of the electrolyte

The synthesis of the biopolymer electrolyte is carried out by the simple solution casting technique. The NaAlg biopolymer is dissolved in DD water at 80 °C with different compositions (40, 35, 30, and 25 M.wt%), to get a homogenous solution. Different concentration of NH_4ClO_4 (60, 65, 70, and 75 M.wt%) are dissolved separately, added to the NaAlg solution at 80 °C and stirred for 2 h to get a homogenous solution. The solution was casted into petri dishes and vacuum evaporated in oven at 60 °C for 12 h. After drying, the free standing transparent films were obtained.

Characterization technique

XRD

The amorphous/crystalline nature of the membrane has been investigated utilizing Cu-Kα radiation at an angle of 2θ = 5⁻80° at a rate of 2°/min using the X'Pert PRO diffractometer.

FTIR

A SHIMADZU — IR Affinity-1 spectrometer was used to record FTIR spectra for biopolymer electrolyte films in the range of 500 to 4000 cm^{-1} with a resolution of 1 cm^{-1} at ambient temperature in order to study the complex formation between the NaAlg biopolymer and the NH_4ClO_4 salt.

DSC analysis

The prepared biopolymer electrolyte's glass transition temperatures were measured using a DSC Q20 V24.10 Build 124 apparatus in nitrogen atmosphere at a temperature range between 10 and 180 °C with a heating rate of 10 °C/min.

TGA analysis

SDT Q600 V20.9 Build 20 has been used to investigate the thermal stability of the biopolymer electrolyte in nitrogen atmosphere at a flow rate of 200 ml/min. In the range of 30 to 700 °C, the samples were heated at a rate of 10 °C/min.

Impedance analysis

Impedance analysis is a useful technique for examining the electrical properties of the biopolymer electrolytes. By sandwiching the biopolymer membrane and using stainless steel as the electrodes, an HIOKI 3532 LCR meter connected to a computer used to measure the impedance of the biopolymer membrane in the frequency range between 42 Hz and 5 MHz.

Linear sweep voltammetry

Using a CHI600C series electrochemical instrument with a scan rate of 0.1 V/s in the range of 0 to 5 V, the highest electrochemical stability window of electrolyte was measured.

Transference number measurement

The polarization current is measured using a DC polarization technique by passing a 1.0 V dc voltage across the configuration of stainless steel (SS)/biopolymer membrane/SS.

Construction of primary battery

A primary proton conducting battery has been fabricated with the configuration, $Zn + ZnSO_4.7H_2O + C$||highest conducting polymer membrane ($30NaAlg + 70NH_4ClO_4$) ||$PbO_2 + V_2O_5 + C$. OCV and discharge performance have been studied with the load resistance of 100 KΩ.

Construction of (PEM) fuel cell

The highest conducting biopolymer electrolyte (30 M.wt%NaAlg:70 M.wt%NH_4ClO_4) has been used to build a PEM fuel cell. OCV and the current drawn for various loads (10 Ω, 270 Ω, and 620 Ω) have been measured.

Results and discussion

XRD

The degree of amorphousness at room temperature has been determined using X-ray diffraction measurements for the biopolymer electrolytes NaAlg with various NH_4ClO_4 concentrations. The XRD patterns are shown in Fig. 2 pure NaAlg curve (a), 40 M.wt% NaAlg:60 M.wt% NH_4ClO_4 curve (b), 35 M.wt% NaAlg:65 M.wt% NH_4ClO_4 curve (c), 30 M.wt% NaAlg:70 M.wt% NH_4ClO_4 curve (d), and 25 M.wt% NaAlg:75 M.wt% NH_4ClO_4 curve (e). The diffraction pattern for pure NaAlg shows a peak at 2θ = 14° and 2θ = 22.8°. These peak positions coincide with the previous results [39, 40]. The diffraction peak at 2θ = 14° disappears for the concentration of 40 NaAlg:60 NH_4ClO_4 (curve (b)), 35 NaAlg:65 NH_4ClO_4 (curve (c)), 30 NaAlg:70 NH_4ClO_4 (curve (d)), and 25 NaAlg:75 NH_4ClO_4 (curve (e)) respectively. The peak at 2θ = 22.8° has become broadened and shifted to 27.7°, 27.4°, and 26.2° for the concentration of 40 NaAlg:60 NH_4ClO_4 (curve (b)), 35 NaAlg:65 NH_4ClO_4 (curve (c)), and 30 NaAlg:70 NH_4ClO_4 (curve (d)) respectively. With an increase in salt concentration, the peak's intensity decreases while its broadness increases. The Hodge et al. criteria, establishing a relationship between peak

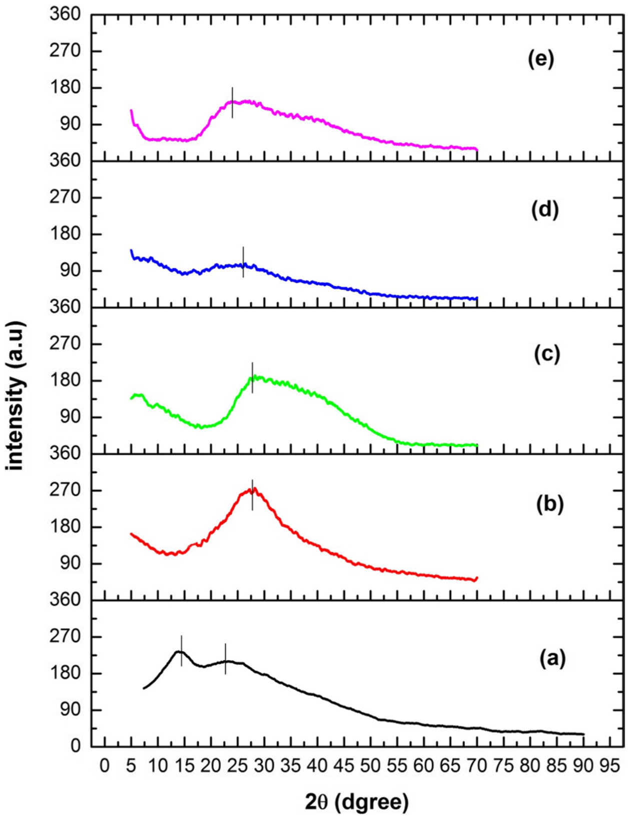

Fig. 2 XRD plot of **a** pure NaAlg, **b** 40NaAlg:60 NH_4ClO_4, **c** 35 NaAlg:65 NH_4ClO_4, **d** 30 NaAlg:70 NH_4ClO_4, and **e** 25 NaAlg:75 NH_4ClO_4

intensity and degree of crystallinity, were used to interpret the results [41]. The maximum broadness is observed for 30 NaAlg:70 NH_4ClO_4 biopolymer membrane, showing that this membrane is more amorphous than other membranes. The peak at $2\theta = 23.2°$ has increased intensity and decreased broadness for the composition of 25 NaAlg:75 NH_4ClO_4 (curve (e)). This shows decline in amorphous nature. The increase in amorphous nature could be explained, whenever salts are added to the polymer, added salt perturbs the polymer network, and produced disorderliness in the network, i.e., amorphousness nature increases. As the concentration of the salt is increased the above process is increases up to a particular concentration of the salt. After the particular concentration, even though salt concentration is increased, the above process, i.e., creation of disorderliness, does not take place.

Figure 3 depicts the deconvoluted XRD plot for pure NaAlg (curve (a)) and different concentration of NaAlg with NH_4ClO_4, 40 NaAlg:60 NH_4ClO_4 (curve (b)), 35 NaAlg:65 NH_4ClO_4 (curve (c)), 30 NaAlg:70 NH_4ClO_4 (curve (d)), and 25 NaAlg:75 NH_4ClO_4 (curve (e)).

$$\text{Crystallinitypercentage} = \frac{\text{Areaundercrystallineregion}}{\text{Totalareaofthepeak}} \times 100$$

The formula has been used to get the crystallinity percentage.

The crystallinity percentages are shown in Table 1. Table 1 shows, the percentage of crystallinity has been

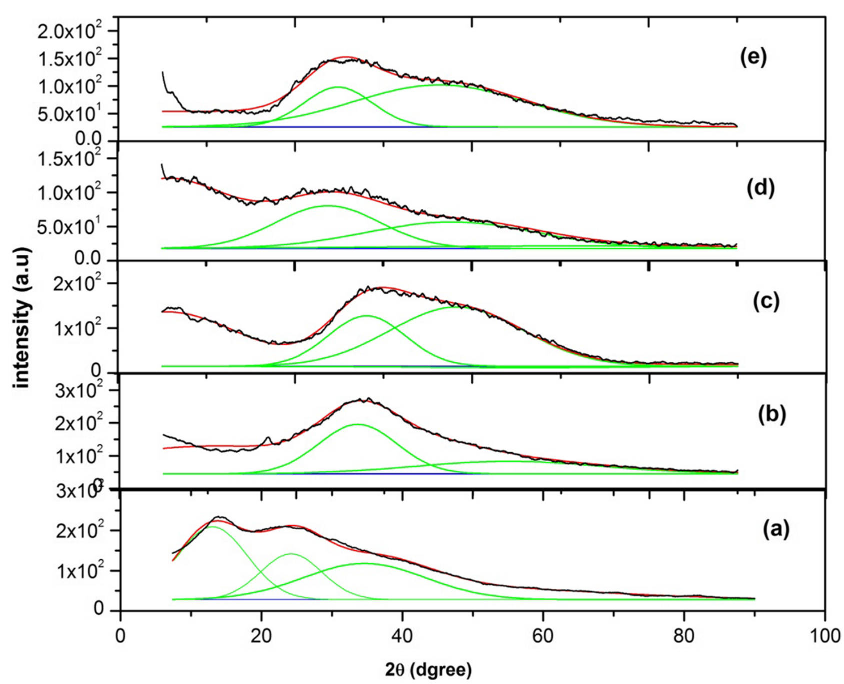

Fig. 3 Deconvoluted XRD plot of **a** pure NaAlg, **b** 40 NaAlg:60 NH_4ClO_4, **c** 35 NaAlg:65 NH_4ClO_4, **d** 30 NaAlg:70 NH_4ClO_4, and **e** 25 NaAlg:75 NH_4ClO_4

Table 1 Crystallinity percentage of the biopolymer membrane

S. No	Compositions	% of crystallinity
1	Pure NaAlg	41.34
2	40 NaAlg:60 NH_4ClO_4	39.61
3	35 NaAlg:65 NH_4ClO_4	26.13
4	30 NaAlg:70 NH_4ClO_4	15.16
5	25 NaAlg:75 NH_4ClO_4	38.19

observed for pure NaAlg as 41.34%. With the addition of NH_4ClO_4 salt the crystallinity percentage decreases to 39.61%, 26.13%, and 15.16% for 40 NaAlg:60 NH_4ClO_4, 35 NaAlg:65 NH_4ClO_4, and 30 NaAlg:70 NH_4ClO_4 respectively. The NaAlg biopolymer membrane has become more amorphous as the salt concentration increased. Further addition of NH_4ClO_4 salt (25 NaAlg:75 NH_4ClO_4) the crystallinity percentage increases to 38.19%. Biopolymer membrane 30 NaAlg:70 NH_4ClO_4 shows a high amorphous nature.

Mechanical properties such as microstrain (ε) and dislocation density (δ) along with crystalline size have been calculated from the XRD data using the formula [42, 43].

The crystalline size (D) has been calculated using Debye–Scherrer formula,

$$D = \frac{k\lambda}{\beta cos\theta}$$

Micro-strain (ε) and dislocation density (δ) are calculated by using the formula,

$$\varepsilon = \frac{\beta cos\theta}{4}$$

$$\delta = \frac{1}{D^2}$$

where k is the Scherrer constant (0.94), λ is the wavelength of the Cu-Kα X-ray radiation (1.54 nm), β is the full width half maximum (FWHM) of the diffraction peak, and θ is the Bragg angle (in radians).

These mechanical properties have been calculated with respect to the prominent peaks at 2θ = 22.8°, 27.7°, 27.4°, 26.2°, and 23.2° for pure NaAlg, 40 NaAlg:60 NH_4ClO_4, 35 NaAlg:65 NH_4ClO_4, 30 NaAlg:70 NH_4ClO_4, and 25 NaAlg:75 NH_4ClO_4 respectively and depicted in Table 2.

Table 2 shows that.

a) Increasing the concentration of salt from 60 M.wt% NH_4ClO_4 to 70 M.wt% NH_4ClO_4 crystalline size have been decreased compare to pure NaAlg.
b) Increasing the concentration of salt 60 M.wt%NH_4ClO_4 to 70 M.wt% NH_4ClO_4 microstrain and dislocation density have been increased compare to pure NaAlg.
c) For 75 M.wt% NH_4ClO_4 with 25 M.wt% NaAlg membrane microstrain and dislocation density have been decreased compare to pure NaAlg.

FTIR

FTIR spectroscopy is used to study the complex formation between the biopolymer NaAlg and the NH_4ClO_4 salt. Figure 4 depicts the FTIR spectra of pure NaAlg. Figure 5 depicts the FTIR spectra of 40 NaAlg:60 NH_4ClO_4, 35 NaAlg:65NH_4ClO_4, 30 NaAlg:70 NH_4ClO_4, and 25

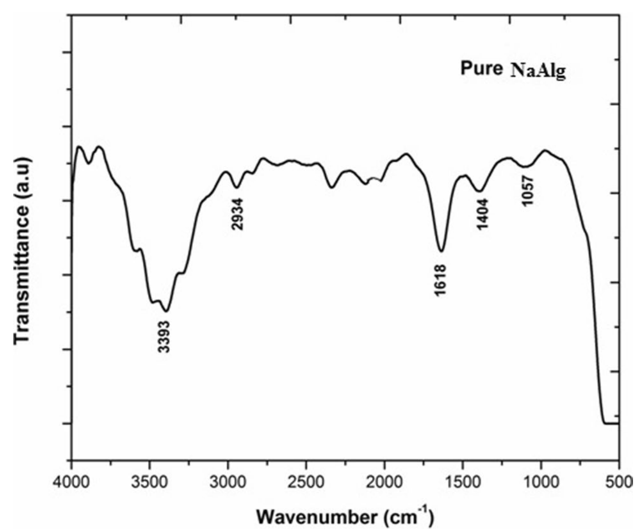

Fig. 4 FTIR spectrum of pure NaAlg

Table 2 Calculated mechanical property for prepared polymer electrolytes from XRD

Composition	2θ (deg.)	Crystalline size D (nm)	Micro-strain ε (10^{-2})	Dislocation density δ (10^{18})
Pure NaAlg	22.8	1.67	2.16	0.35
40 NaAlg:60NH_4ClO_4	27.7	1.45	2.49	0.48
35 NaAlg:65 NH_4ClO_4	27.4	1.42	2.54	0.50
30 NaAlg:70 NH_4ClO_4	26.2	1.06	3.40	0.89
25 NaAlg:75 NH_4ClO_4	23.2	2.32	1.55	0.19

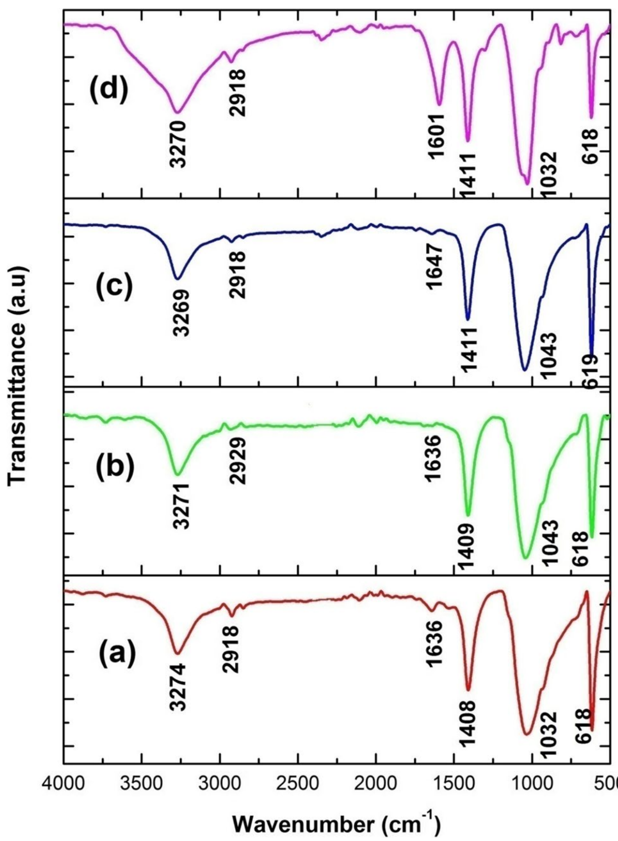

Fig. 5 FTIR spectrum of **a** 40 NaAlg:60 NH_4ClO_4, **b** 35 NaAlg:65 NH_4ClO_4, **c** 30 NaAlg:70 NH_4ClO_4, and **d** 25 NaAlg:75 NH_4ClO_4

NaAlg:75 NH_4ClO_4, and Table 3 shows the corresponding vibrational peaks that were assigned.

The IR peak in the pure NaAlg at 1057 cm^{-1} is associated with C–O–C stretching. This peak vibration gets shifted to 1032 cm^{-1}, 1043 cm^{-1}, 1043 cm^{-1}, and 1032 cm^{-1} for the biopolymer electrolytes 40 NaAlg:60 NH_4ClO_4, 35 NaAlg:65 NH_4ClO_4, 30 NaAlg:70 NH_4ClO_4, and 25 NaAlg:75 NH_4ClO_4 respectively which reveals the coordination between salt and biopolymer.

The peak 1404 cm^{-1} is assigned to COO^- symmetric stretching for pure NaAlg and on incorporation of different concentrations of the salt to the biopolymer membrane the peak gets shifted to 1408 cm^{-1}, 1409 cm^{-1}, 1411 cm^{-1}, and 1411 cm^{-1} for the biopolymer electrolytes 40 NaAlg:60 NH_4ClO_4, 35 NaAlg:65 NH_4ClO_4, 30 NaAlg:70 NH_4ClO_4, and 25 NaAlg:75 NH_4ClO_4 respectively.

The peak at 1618 cm^{-1} in pure NaAlg represents COO^- asymmetric stretching [21]. And this peak is absent for 40 NaAlg:60 NH_4ClO_4, 35 NaAlg:65 NH_4ClO_4, and 30 NaAlg:70 NH_4ClO_4 membranes.

A peak at 1601 cm^{-1} is observed for 25 NaAlg:75 NH_4ClO_4 this may be due to COO^- asymmetric stretching [23].

Appearance of the peak around 1601 cm^{-1} is assigned to COO^- asymmetric stretching by other people. So it is shows that for higher concentration asymmetric peak appears again. Appearance and disappearance of a particular peak may lead to the understanding that complex formation has been formed between the salt and polymer.

The C-H stretching appears at 2934 cm^{-1} for pure NaAlg. When the salt is incorporated in the polymer matrix the peak is shifted to 2918 cm^{-1}, 2929 cm^{-1}, 2918 cm^{-1}, and 2918 cm^{-1} for 40 NaAlg:60 NH_4ClO_4, 35 NaAlg:65 NH_4ClO_4, 30 NaAlg:70 NH_4ClO_4, and 25 NaAlg:75 NH_4ClO_4 respectively. The intensity of the peak gets reduced on adding different salt concentration.

For pure NaAlg, the O–H stretching peak appears at 3393 cm^{-1}. And the peak is shifted to 3274 cm^{-1}, 3271 cm^{-1}, 3269 cm^{-1}, and 3270 cm^{-1} for 40 NaAlg:60 NH_4ClO_4, 35 NaAlg:65 NH_4ClO_4, 30 NaAlg:70 NH_4ClO_4, and 25 NaAlg:75 NH_4ClO_4 respectively.

Table 3 FTIR peak assignments of NaAlg biopolymer with NH_4ClO_4 salt

S. No	Pure NaAlg	40NaAlg:60NH_4ClO_4	35NaAlg:65NH_4ClO_4	30NaAlg:70NH_4ClO_4	25NaAlg:75NH_4ClO_4	Assignment	Reference
1	-	618	618	619	618	ClO_4^- stretching	[44, 45]
2	1057	1032	1043	1043	1032	C–O–C stretching	[12, 46]
3	1404	1408	1409	1411	1411	COO^- symmetric stretching	[23, 38, 47]
4	1618	1636	1636	1647	1601	COO^- asymmetric stretching	[21, 23]
5	2934	2918	2929	2918	2918	C-H stretching	[48, 49]
6	3393	3274	3271	3269	3270	O–H stretching	[37, 50]

The new peaks 618 cm^{-1}, 618 cm^{-1}, 620 cm^{-1}, and 619 cm^{-1} occurred for 40 NaAlg:60 NH_4ClO_4, 35 M.wt%NaAlg:65 NH_4ClO_4, 30 NaAlg:70 NH_4ClO_4, and 25 NaAlg:75 NH_4ClO_4 respectively are due to the ClO_4^- stretching.

Using the given formula calculate the force constant (k) value,

$$\overline{\upsilon} = \frac{1}{2\pi c}\sqrt{\frac{k}{\mu}}\text{cm}^{-1} \quad (1)$$

where $\bar{\upsilon}$ is the wave number (cm^{-1}), c is the velocity of light (3×10^{10} cm s^{-1}), k is the force constant (N/cm), μ is the reduced mass ($\mu = \frac{m_1\times m_2}{m_1+m_2}$), m_1 is the atomic mass of O, m_2 is the atomic mass of H.

The force constant values are shown in Table 4. As shown in Table 4, the force constant values decreases with an increase in the composition of 40 NaAlg:60 NH_4ClO_4, 35 NaAlg:65 NH_4ClO_4, 30 NaAlg:70 NH_4ClO_4, and 25 NaAlg:75 NH_4ClO_4. This decrease of force constant shows that decreases frequency with an increase in bond length. The possible interaction between NH_4ClO_4 with the NaAlg is shown in Fig. 6.

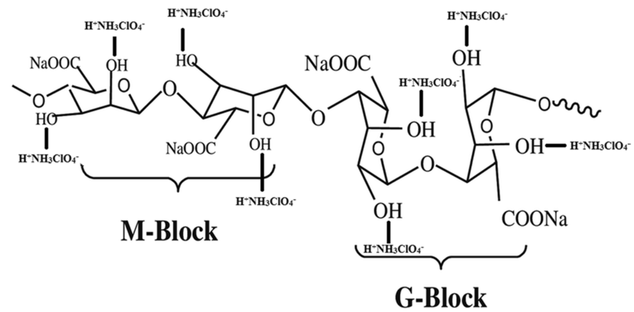

Fig. 6 Possible interaction of NH_4ClO_4 salt with NaAlg biopolymer

DSC

The T_g (glass transition temperature) of the biopolymer electrolytes has been evaluate by the DSC analysis. Figure 7 shows the DSC thermogram of pure NaAlg and different M.wt% of NaAlg with NH_4ClO_4 salt (40 NaAlg:60 NH_4ClO_4, 35 NaAlg:65 NH_4ClO_4, 30 NaAlg:70 NH_4ClO_4, and 25 NaAlg:75 NH_4ClO_4). Figure 7a depicts the pure NaAlg and it exhibits a T_g value of 52.8 °C. With Addition of ammonium salt the T_g value decreases to 41.81 °C, 40.56 °C, and 38.62 °C for 40 NaAlg:60 NH_4ClO_4, 35 NaAlg:65 NH_4ClO_4, and 30 NaAlg:70 NH_4ClO_4 respectively. Addition of the salt stimulates the rubbery state in the biopolymer electrolytes which is indicated by the decrease in the glass transition temperature (T_g). The rubbery state leads to more flexible nature. High ionic conductivity is expected for the sample 30 NaAlg:70 NH_4ClO_4. On further increasing of salt concentration 25 NaAlg:75 NH_4ClO_4 the T_g value increases to 41.3 °C. This increase in T_g is caused by the aggregates formation of ions, which reduces the flexibility of the polymer chain. Moniha et al. [51] found similar result for the composition of i-carrageenan with NH_4SCN, while Maheshwari et al. reported similar result for the composition of dextran:PVA:NH_4NO_3 [52].

Table 4 Force constant values of NaAlg biopolymer with NH_4ClO_4 for O–H stretching

Composition	Wavenumber (cm^{-1})	Force constant (N cm^{-1})
Pure NaAlg	3393	638.68
40 NaAlg:60 NH_4ClO_4	3274	594.67
35 NaAlg:65 NH_4ClO_4	3271	593.58
30 NaAlg:70 NH_4ClO_4	3169	557.14
25 NaAlg:75 NH_4ClO_4	3170	557.49

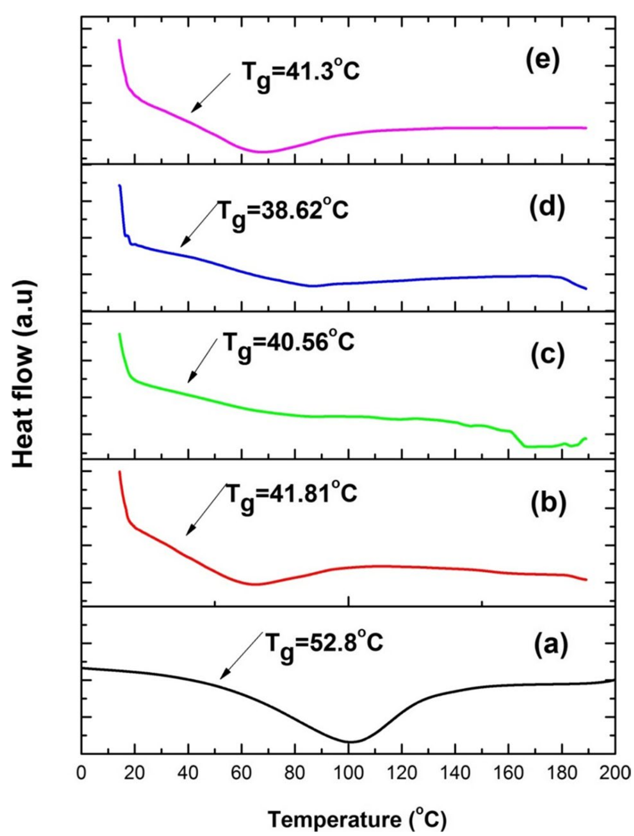

Fig. 7 DSC thermogram of **a** pure NaAlg, **b** 40 NaAlg:60 NH_4ClO_4, **c** 35 NaAlg:65 NH_4ClO_4, **d** 30 NaAlg:70 NH_4ClO_4, and **e** 25 NaAlg:75 NH_4ClO_4

TGA

The thermograms of pure NaAlg and 30 NaAlg:70 NH_4ClO_4 are shown in Fig. 8. Table 5 depicts the three different decomposition stages which occur in the 30 to 700 °C temperature range.

The initial weight loss occurs by moisture evaporating from the polymer electrolytes in the pure NaAlg (30–70 °C, 9.8% weight loss) and 30 NaAlg:70 NH_4ClO_4 (30–74 °C, 6.6% weight loss).

Pure NaAlg decomposes at 71–210 °C with an 8.2% weight loss during the first stage, and the weight loss occurs by moisture evaporation and the residual solvent in the polymer electrolyte. The weight loss in the first stage of 30 NaAlg:70 NH_4ClO_4 (75–191 °C, 6.3% weight loss) is caused by salt decomposition and residual solvent evaporation.

For pure NaAlg (211–268 °C, 35% weight loss) and 30 NaAlg:70 NH_4ClO_4 (192–355 °C, 58.8% weight loss), the weight loss in the second stage of decomposition is caused by the loss of the carboxylate group from the polymer backbone.

For pure NaAlg (269–700 °C, 17% weight loss) and 30 NaAlg:70 NH_4ClO_4 (356–691 °C, 11.1% weight loss), weight loss occurs through carbonization and the formation of ash during the third decomposition stage.

Similar findings have been reported by Fuzlin et al. for the biopolymers alginate with NH_4Br and NaAlg with glycolic acid as well as by Vanitha et al. for the biopolymer NaAlg with NH_4SCN [5, 26, 38].

Impedance analysis

Impedance spectroscopy has been used to measure the ionic conductivity of the prepared biopolymer electrolytes. Figure 9 shows the Nyquist plot for pure NaAlg and various concentration of NaAlg with NH_4ClO_4 salt (40 NaAlg:60 NH_4ClO_4, 35 NaAlg:65 NH_4ClO_4, 30 NaAlg:70 NH_4ClO_4, and 25 NaAlg:75 NH_4ClO_4) and its equivalent circuit.

Figure 9a for pure NaAlg shows a high frequency semicircle and a low frequency spike. The high frequency semicircle arises due to the parallel combination of bulk capacitance (C_p)

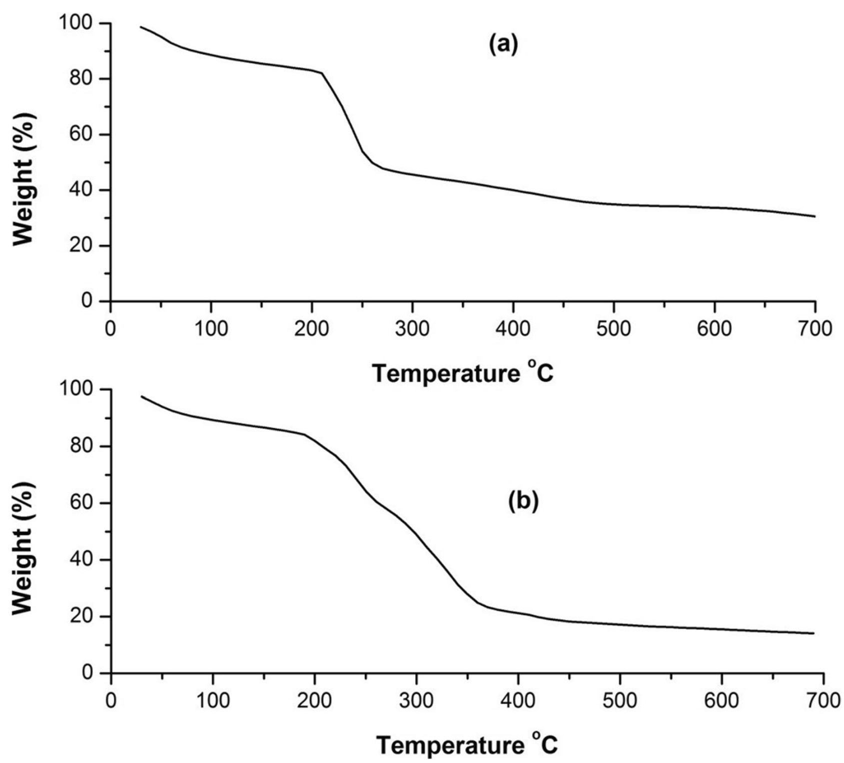

Fig. 8 TGA thermogram for **a** pure NaAlg and **b** 30 NaAlg:70 NH_4ClO_4

Table 5 Thermal properties of biopolymer electrolyte

Sample	Temperature (°C)				Weight loss (%)			
	Initial stage	I stage	II stage	III stage	Initial stage	I stage	II stage	III stage
Pure NaAlg	30–70	71–210	211–268	269–700	9.8	8.2	35	17
30 NaAlg:70 NH_4ClO_4	30–74	75–191	192–355	356–691	6.6	6.3	58.8	11.1

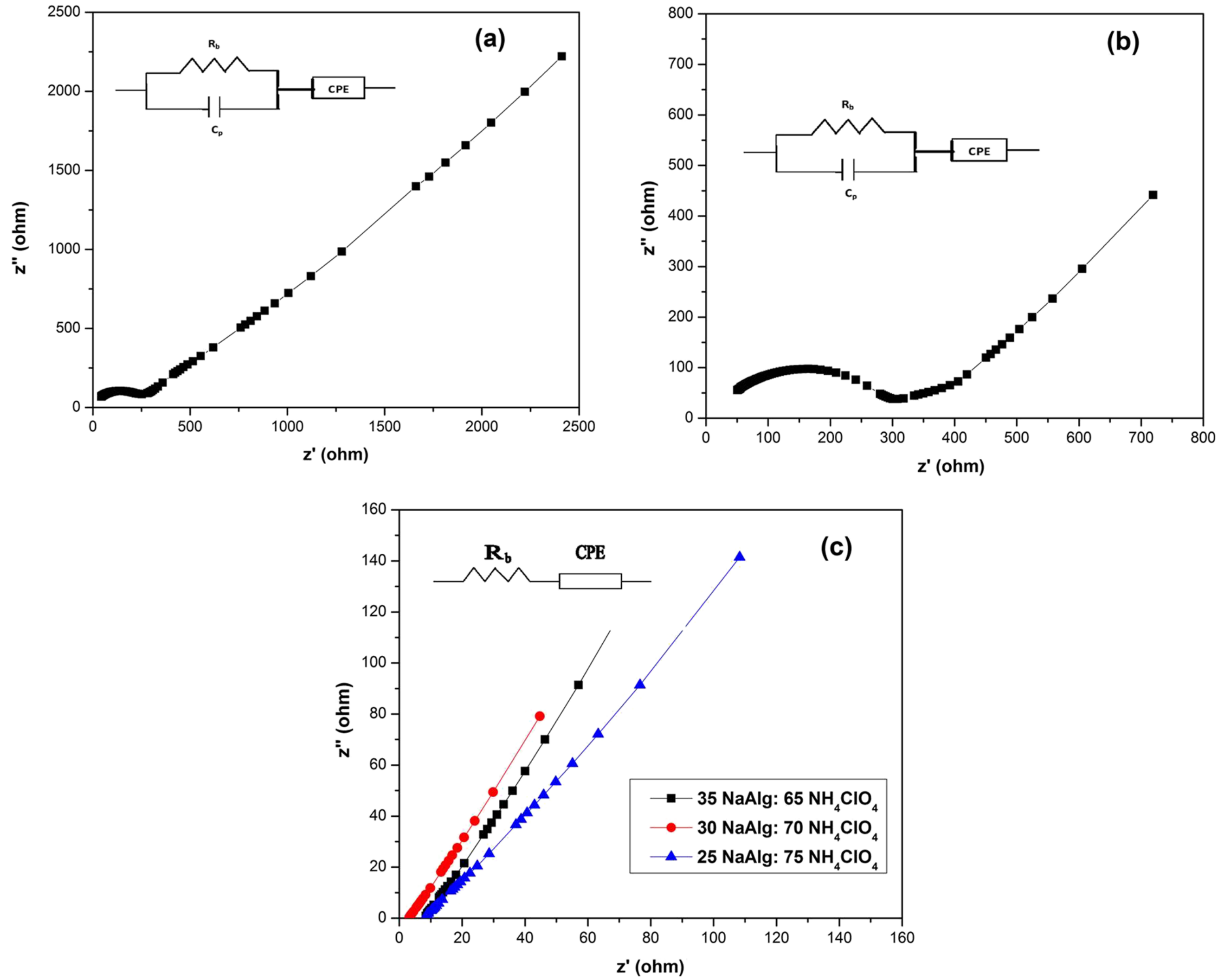

Fig. 9 Nyquist plot for **a** pure NaAlg and equivalent circuit, **b** 40 NaAlg:60 NH_4ClO_4 and equivalent circuit, **c** 35 NaAlg:65 NH_4ClO_4, 30 NaAlg:70 NH_4ClO_4, and 25 NaAlg:75 NH_4ClO_4 and equivalent circuit

and bulk resistance (R_b) of the material and low frequency spike is due to electrode–electrolyte interface [53]. The bulk capacitance (C_p) is frequency dependent one. With the addition of NH_4ClO_4 salt to pure NaAlg, Fig. 9b of 40 NaAlg:60 NH_4ClO_4 shows a semicircle with spike. Figure 9c of 35 NaAlg:65 NH_4ClO_4, 30 NaAlg:70 NH_4ClO_4, and 25 NaAlg:75 NH_4ClO_4 shows the disappearance of the semicircle. Within the frequency range studied, the biopolymer electrolyte has only a dominant resistive component. Using the relation,

$$\sigma = \frac{l}{AR_b} Scm^{-1}$$

where l, A is the thickness and area of the biopolymer membrane, R_b is the bulk resistance of the biopolymer membrane.

The ionic conductivity (σ) is calculated for all the compositions at room temperature, and the results are shown in Table 6. From Table 6, the biopolymer electrolyte of 30 NaAlg:70 NH_4ClO_4 has a very high number of charge carriers, which produces a highest ionic conductivity value of 3.59×10^{-3} S cm^{-1} at ambient temperature. And this membrane has got more amorphous nature (confirmed by XRD) and also low T_g value (confirmed by DSC).

Using Boukamp software, the R_b value of the biopolymer membrane has been measured [54]. EIS parameter values of the biopolymer membrane are tabulated in Table 7. From Table 7, R_b value is 6.35×10^3 Ω for pure NaAlg. For 40 NaAlg:60 NH_4ClO_4, 35 NaAlg:65 NH_4ClO_4, and 30 NaAlg:70 NH_4ClO_4 and 25 NaAlg:75 NH_4ClO_4 biopolymer electrolytes, the R_b value has decreased 3.32×10^3 Ω, 2.81×10^2 Ω, and 1.02×10^1 Ω respectively. For the composition of 25 NaAlg:75 NH_4ClO_4, the R_b value increased to 2.08×10^2 Ω. Constant phase element (CPE) impedance can be calculated using,

Table 6 Ionic conductivity value for the prepared biopolymer electrolytes at 303 K

Polymer composition	Conductivity σ (S cm^{-1})
Pure NaAlg	9.11×10^{-6}
40 NaAlg:60 NH_4ClO_4	1.59×10^{-5}
35 NaAlg:65 NH_4ClO_4	9.98×10^{-4}
30 NaAlg:70 NH_4ClO_4	3.59×10^{-3}
25 NaAlg:75 NH_4ClO_4	9.82×10^{-4}

Table 7 EIS parameters of the biopolymer electrolytes

S. No	Compositions	R_b (ohm)	*CPE* (μF)	*n* (no unit)
1	Pure NaAlg	6.35×10^{3}	1.49×10^{-5}	1.87
2	40 NaAlg:60 NH_4ClO_4	3.32×10^{3}	8.72×10^{-6}	0.37
3	35 NaAlg:65 NH_4ClO_4	2.81×10^{2}	1.29×10^{-5}	0.42
4	30 NaAlg:70 NH_4ClO_4	1.02×10^{1}	1.98×10^{-3}	0.74
5	25 NaAlg:70 NH_4ClO_4	2.08×10^{2}	3.42×10^{-4}	0.52

$$Z_{CPE} = \frac{1}{Q_0(j\omega)^n}$$

where n, Q_0 is the frequency independent factor

The value of n is 1, shows pure capacitor, and n is 0, shows the pure resistor [55]. The CPE value for pure NaAlg is 1.49×10^{-5} μF. On adding of NH_4ClO_4 salt with NaAlg, 40 NaAlg:60 NH_4ClO_4, 35 NaAlg:65 NH_4ClO_4, 30 NaAlg:70 NH_4ClO_4 and 25 NaAlg:75 NH_4ClO_4, the CPE value were 8.72×10^{-6} μF, 1.29×10^{-5} μF, 1.98×10^{-3} μF, and 3.42×10^{-4} μF respectively. Pure NaAlg has an n value of 1.87. For various concentration of salt NH_4ClO_4 with NaAlg, 40 NaAlg:60 NH_4ClO_4, 35 NaAlg:65 NH_4ClO_4, 30 NaAlg:70 NH_4ClO_4, and 25 NaAlg:75 NH_4ClO_4, the values of n were 0.37, 0.42, 0.74, and 0.52 respectively. The composition of 25 NaAlg:75 NH_4ClO_4, the conductivity value decreases to 9.82×10^{-4} S cm^{-1} and is due to salt aggregate formation.

Selvin et al. have observed a conductivity of 6.83×10^{-4} S cm^{-1} for the composition of 1-g κ-carrageenam with 0.5% NH_4SCN [25]. Rasali et al. have obtained a maximum conductivity of 5.56×10^{-5} S cm^{-1} for the composition of 2-g alginate:25wt% NH_4NO_3 [56]. Moniha et al. reported that the conductivity value of 1.46×10^{-3} S cm^{-1} for 1-g i-carrageenam:0.4wt% NH_4NO_3 [57]. According to Monisha et al., maximum conductivity value was 1.02×10^{-3} S cm^{-1} for 50 mol% cellulose acetate:50 mol% NH_4NO_3 [58].

Conductance spectra

Conductance spectra of pure NaAlg and different composition of 40 NaAlg:60 NH_4ClO_4, 35 NaAlg:65 NH_4ClO_4, 30 NaAlg:70 NH_4ClO_4, and 25 NaAlg:75 NH_4ClO_4 are shown in Fig. 10. Usually, the conduction spectra is characterized by three regions. The first region is low-frequency dispersive region, which relates to the polarization of the electric charge at the interface between the electrode and the electrolyte [59]. The second is a mid-frequency independent plateau region, which is related to the DC conductivity of the prepared biopolymer electrolyte. Finally, the third is the high frequency region, which relates to the bulk relaxation process of the biopolymer electrolyte. Only the low frequency and mid frequency bands are observed in this work. The AC conductivity spectra show that the conductivity increases with increasing salt concentration, which is associated with the increase in charge carriers. The dc conductivity (σ_{dc}) values for all the biopolymer electrolytes are obtained by extrapolating the plateau region to the log σ axis. It was observed that the conductivity values obtained from the conduction spectra and the Nyquist plot are similar.

Transference number measurement

The Wagner's polarization technique is used to measure the transference number, which determines whether the conductivity in the biopolymer electrolyte is caused by the presence of ions or electrons [60]. Using the formula, the transference number is measured.

$$t_{ion} = \frac{I_i - I_f}{I_i}$$

$$t_{ele} = \frac{I_f}{I_i}$$

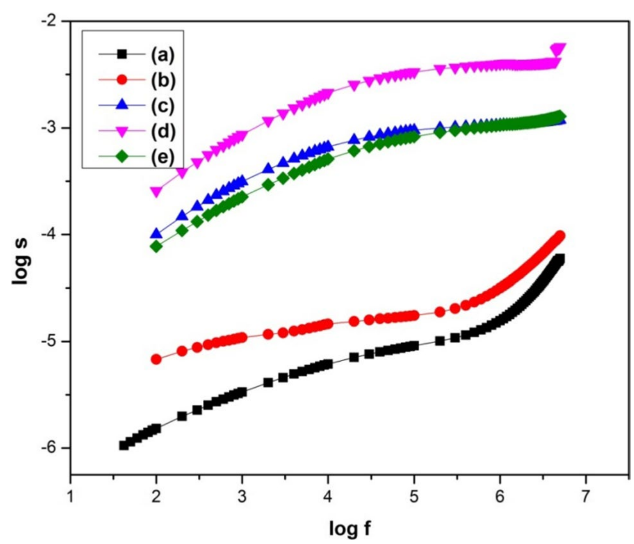

Fig. 10 Conductance spectra for pure NaAlg and NaAlg with various compositions of NH_4ClO_4. **a** Pure NaAlg, **b** 40 NaAlg:60 NH_4ClO_4, **c** 35 NaAlg:65 NH_4ClO_4, **d** 30 NaAlg:70 NH_4ClO_4, and **e** 25 NaAlg:75 NH_4ClO_4

where I_i, I_f is the initial and final current.

In this technique a dc potential of 1.0 V was applied across the cell of the stainless steel (SS):30 NaAlg with 70 NH_4ClO_4:SS configuration for polarization and after polarization. The initial current decreases with time as shown in Fig. 11 and reaches a constant value in the fully depleted situation due to the depletion of ionic species in the biopolymer electrolyte [61]. Using transference number equation, the t_{ele} and t_{ion} for the highest conducting biopolymer electrolyte (30 NaAlg:70 NH_4ClO_4) is observed to be 0.019 and 0.98 which is nearly unity which ensures that the charge transport is mainly due to ions and hence these electrolytes are suitable for solid-state electrochemical cells. Meera Nachiyar et al. have reported that the value of t_{ion} as 0.95 for the composition 1.0-g gellan gum with 0.9 M.wt% of NH_4HCO_2 [37]. The value of t_{ion} reported by Maheshwari et al. for the composition 700-mg dextran:300-mg PVA:450-mg NH_4NO_3 is 0.99 [52]. Muthukrishnan et al. [35] have reported that the value of t_{ion} 0.962 for 50 M.wt% pectin:50 M.wt% NH_4HCO_2 polymer electrolytes.

LSV

The electrochemical stability of the biopolymer membrane has been examined using the linear sweep voltammetry (LSV) method. The highest conducting biopolymer electrolyte placed between two stainless steel electrodes. Figure 12 illustrates the linear sweep voltammogram of the highest conducting membrane (30 NaAlg:70 NH_4ClO_4). Figure 12 shows that the electrochemical stability is stable up to 2.71 V and further decomposition occurred in the biopolymer electrolyte. Meera Naachiyar et al. have reported the electrochemical window of 2.53 V for 1-g GG:0.9 M.wt% NH_4HCO_2 [37]. Muthukrishnan et al. have obtained electrochemical window of 1.97 V and 2.35 V for 50 M.wt% pectin:50 M.wt% NH_4HCO_2 and 50 M.wt% pectin:50 M.wt% NH_4HCO_2:0.4 wt% EC [35]. Selvalakshmi et al. observed electrochemical stability windows of 2.4 V and 2.5 V for 50 M.wt% agar:50 M.wt% NH_4Br and 50 M.wt% agar:50 M.wt% NH_4I, respectively [27, 62].

Construction of a proton conducting battery

The highest conducting biopolymer electrolyte has been used to develop a primary proton battery (30 NaAlg: 70 NH_4ClO_4) to assess the practical utility of the material. PbO_2, V_2O_5, and C (graphite) in the ratio 4:1:0.5 as cathode in pellet form whereas Zn powder, $ZnSO_4$, and C in the ratio 3:1:1 are used as the anode [63]. The highest conducting biopolymer electrolyte 30 NaAlg:70 NH_4ClO_4 is placed in the battery holder between the anode and cathode pellets. Figure 13 depicts the schematic diagram of the constructed battery. The battery configuration is

$$Zn + ZnSO_4.7H_2O + C|30NaAlg : 70NH_4ClO_4|PbO_2 + V_2O_5 + C$$

The chemical reaction taking place in the battery cell are characterised as follows:

The anode reaction is

$$Zn \rightarrow Zn^{2+} + 2e^-$$

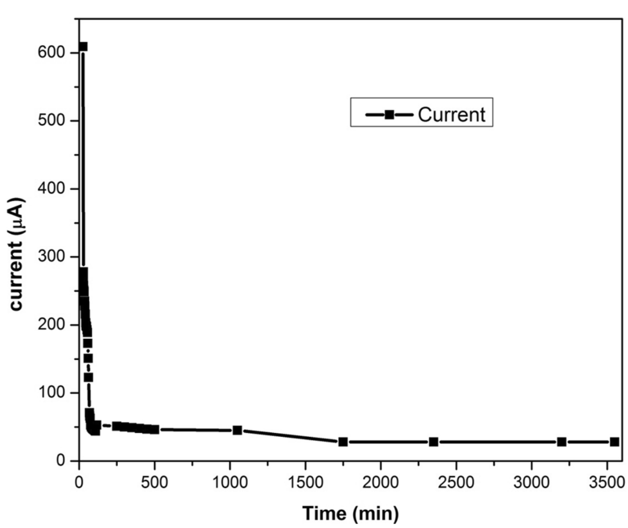

Fig. 11 Variation of DC with time for 30 NaAlg:70 NH_4ClO_4 (highest conducting electrolyte) using Wagner's method

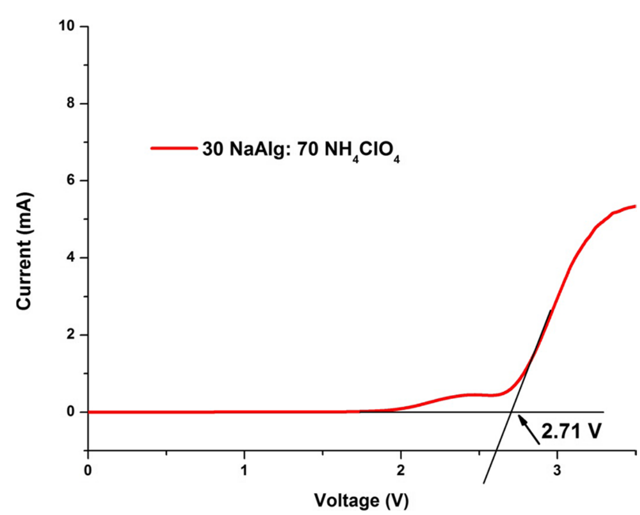

Fig. 12 Linear sweep voltammetry recorded for 30 NaAlg:70 NH_4ClO_4

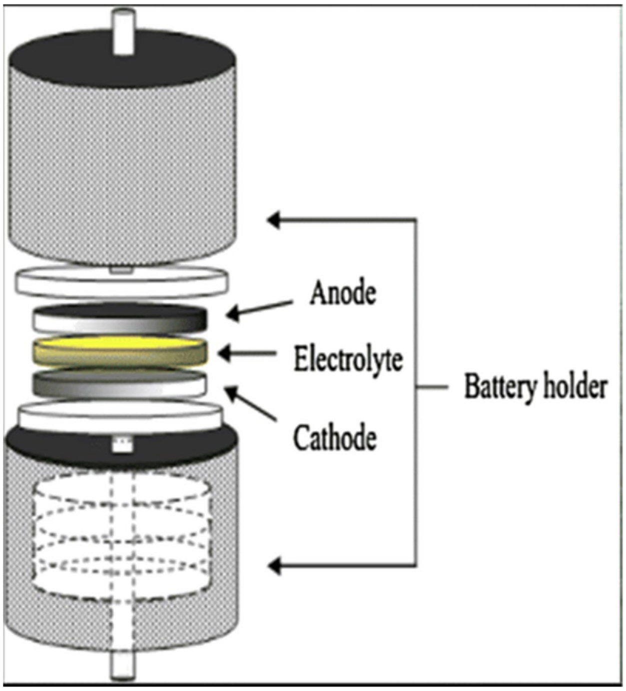

Fig. 13 Configuration of battery

The cathode reaction is

$$PbO_2 + 4H^+ + 2e^- \rightarrow Pb^{2+} + 2H_2O$$

$$V_2O_5 + 6H^+ + 2e^- \rightarrow 2VO^{2+} + 3H_2O$$

The initial V_{oc} is monitored with respect to time and recorded as 1.76 V (Fig. 14), and it is observed for 60 h. The external load of 100 KΩ is applied across the cell. The initial cell potential value decreases from 1.76 to 1.71 V, and the current of 17 μA is drawn. After discharging, the voltage steadily drops and remains constant at 1.24 V for 60 h (Fig. 14). Figure 15 shows the V_{oc}. Table 8 provides the values for the cell parameters.

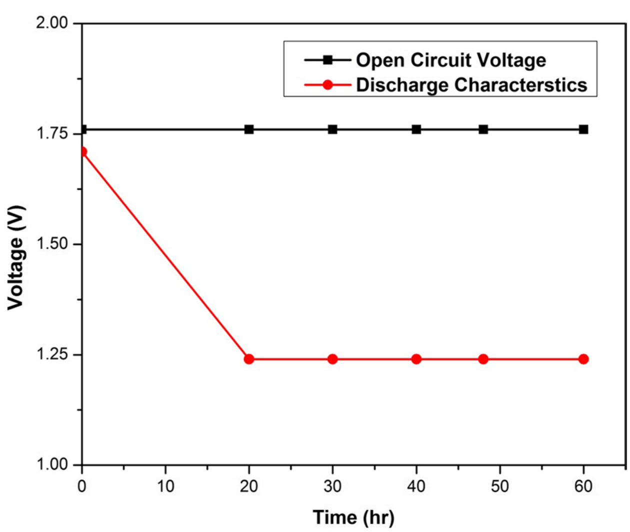

Fig. 14 Open circuit voltage and discharge characteristic curve for the cell

Fig. 15 Open Circuit Voltage for 30 NaAlg: 70 NH_4ClO_4

Muthukrishan et al. have reported a V_{oc} of 1.48 V for 30 M.wt% pectin:70 M.wt% NH_4I [34]. Maheshwari et al.

Table 8 Cell parameters

S. No	Cell parameters	30 NaAlg:70 NH_4ClO_4
1	Open circuit voltage (OCV)	1.76 V
2	Current drawn	17 μA
3	Weight of the cathode	0.716 g
4	Weight of the anode	0.592 g
5	Weight of the electrolyte	0.114 g
6	Weight of the cell	1.422 g
7	Thickness of the anode	1.362
8	Thickness of the cathode	1.356
9	Area of the cell	1.143 cm^2
10	Discharge time	60 h

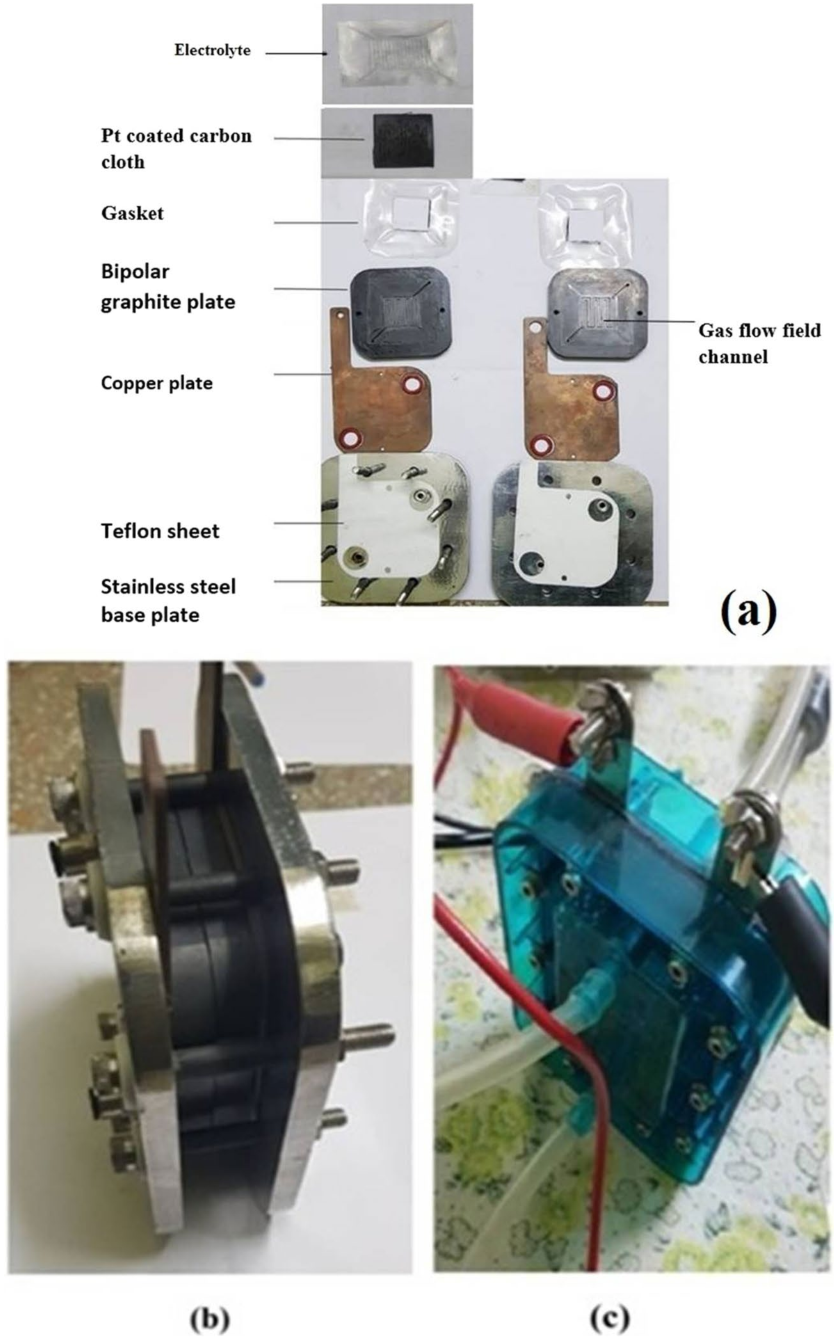

Fig. 16 **a** Parts of fuel cell, **b** constructed single stack fuel cell, **c** electrolyser

have reported for the composition of 700-mg dextran:300-mg PVA:450 mg NH_4NO_3 system a V_{oc} of 1.51 V [52]. Meera Naachiyar et al. reported a V_{oc} of 1.62 V for 1-g gellan gum:1.1 M.wt% NH_4SCN [64].

Fabrication of PEM fuel cell

The PEM fuel cell has been developed in accordance with the techniques used by Monisha et al. [58]. A hand-tightened membrane electrode assembly (MEA), bipolar graphite plates, teflon sheets, thin gaskets, copper plates, and stainless steel plates compose the PEM fuel cell. Figure 16a shows the parts of the fuel cell. Teflon sheet is used as an insulator between the stainless steel base plate and the copper plate. Copper plates are typically used as current collectors in PEM fuel cells due to its strong electrical and thermal conductivity and weak corrosion resistance [65]. The copper plate is kept on top of the bipolar graphite plate. A serpentine flow channel [65] with a surface area of 7.84 cm^2 is seen in the bipolar graphite plate. To assemble the hand-tightened MEA, the highest conducting biopolymer membrane (30 NaAlg:70 NH_4ClO_4) has been placed between the catalyst. The catalyst is a platinum-coated carbon cloth with

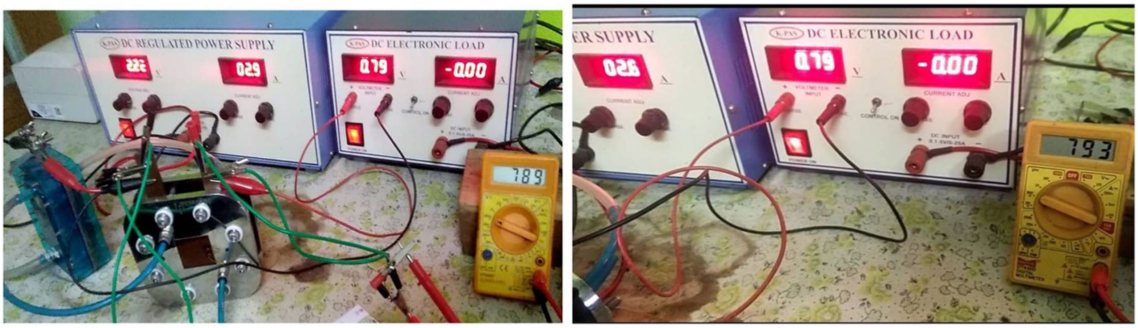

(a) **(b)**

Fig. 17 OCV of single PEM fuel cell for **a** 30 NaAlg:70 NH_4ClO_4 and **b** Nafion.™ 212

Table 9 Current and voltage for various load connected in the fuel cell (30 NaAlg:70 NH_4ClO_4 and Nafion™ 212)

S. No	Load (Ω)	At the instant of connecting load				After 15 min			
		30 NaAlg:70 NH_4ClO_4		Nafion™ 212		30 NaAlg:70 NH_4ClO_4		Nafion™ 212	
		Voltage (mV)	Current (mA)	Voltage (mV)	Current (mA)	Voltage (mV)	Current (mA)	Voltage (mV)	Current (mA)
1	620	778	1.16	766	1.23	622	0.98	773	1.23
2	270	733	2.51	764	2.69	502	1.75	765	2.69
3	10	506	19.49	620	56	252	11.77	631	57

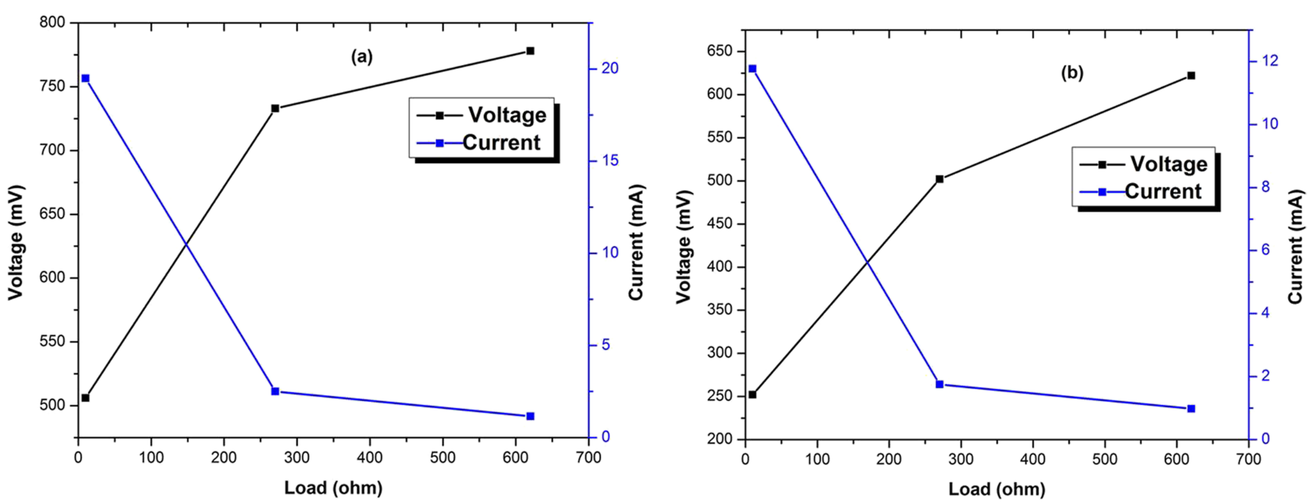

Fig. 18 Variation of current and voltage for various loads (620 Ω, 270 Ω, and 10 Ω) for 30 NaAlg:70 NH_4ClO_4 **a** at instant and **b** after 15 min

a surface area of 8.41 cm^2 that has been evenly coated with platinum at a rate of 0.3 mg/cm^2. This MEA was sandwiched between two bipolar graphite plates with 0.2-mm-thick gaskets. The bipolar graphite plate with MEA has been tightened using gaskets to enhance the flow. The constructed single stack proton exchange membrane (PEM) fuel cell is shown in Fig. 16b.

The electrolyzer has been used to produce the hydrogen and oxygen gases (Fig. 16c). It is operated by a 2-V DC power supply. This electrolyzer supplies 80 ml of oxygen and 100 ml of hydrogen into the PEM fuel cell. When the hydrogen molecule passes over the platinum-coated carbon catalyst, it splits into protons and electrons. The electron flows through the external circuit. The proton crosses the membrane and reaches on the other side, where it combines with an oxygen molecule to produce water. Overall reactions are PEM fuel cell is given below.

$$\text{Anodereactions}: 2H_2 \rightarrow 4H^+ + 4e^-$$

$$\text{Cathodereactions}: O_2 + 4H^+ + 4e^- \rightarrow 2H_2O$$

$$\text{Overallreactions}: 2H_2 + O_2 \rightarrow 2H_2O$$

The PEM fuel cell fabricated using highest conducting biopolymer electrolyte (30 NaAlg:70 NH_4ClO_4) shows the V_{oc} of 789 mV, which is shown in Fig. 17a. The V_{oc} 763 mV and 580 mV have been reported by Meera Naachiyar et al. for gellan gum with NH_4HCO_2 and gellan gum with NH_4SCN [37, 64]. Vanitha et al. have been reported the V_{oc} of 431 mV for NaAlg with NH_4SCN; similarly for NaAlg with NH_4HCO_2 is 707 mV [26, 38]. The V_{oc} for i-carrageenan is combined with NH_4NO_3 has been shown by Moniha et al. to be 442 mV [57]. V_{oc} of 656 mV for CA with ammonium nitrate has been found by Monisha et al. [58].

The PEM fuel cell is connected to several loads such as 10 Ω, 270 Ω, and 620 Ω. For 15 min, each load connects to the fuel cell. At the initial and after 15 min, the current and voltage are measured. After that, the load was removed, and the fuel cell was given time to stabilize. Then connecting the other load, current, and voltage are measured initially and after 15 min. Each load repeats this process. The value of voltage and current for different loads are shown in Table 9. The voltage and corresponding current plotted as graph (Fig. 18).

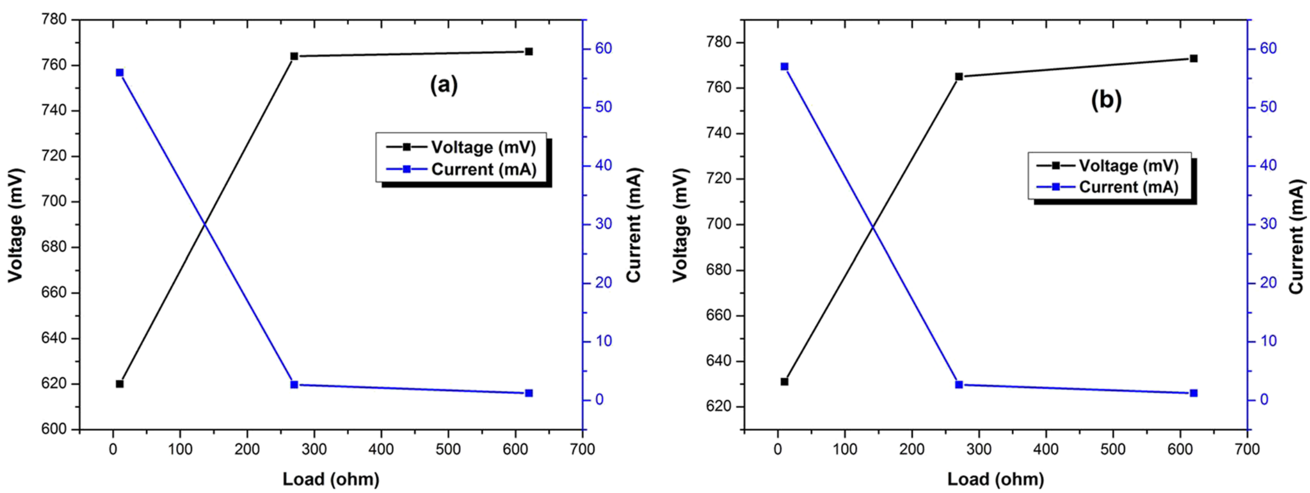

Fig. 19 Variation of current and voltage for various loads (620 Ω, 270 Ω, and 10 Ω) for Nafion™ 212. **a** At instant and **b** after 15 min

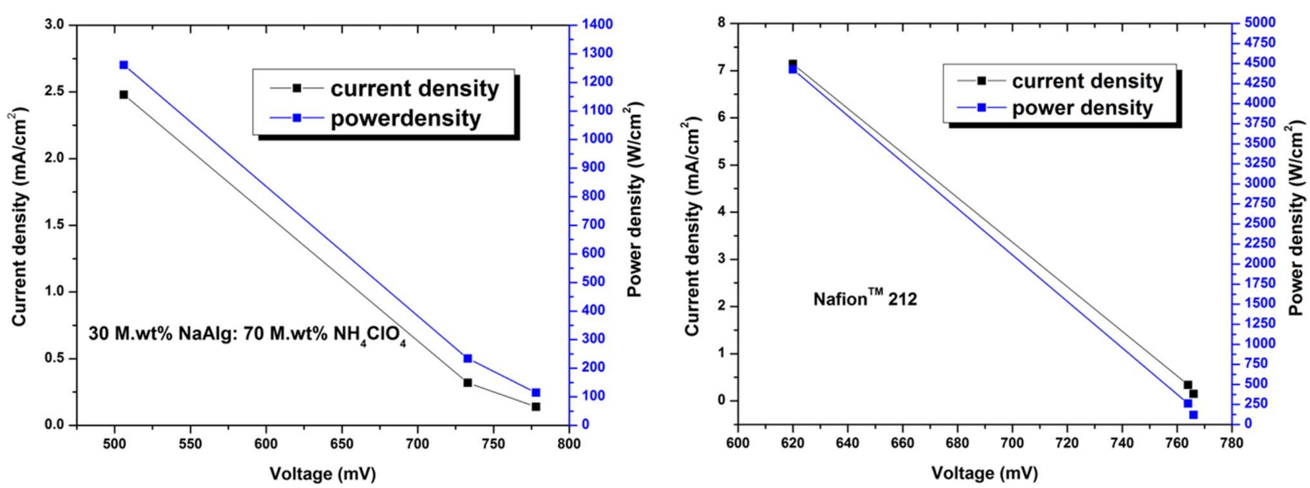

Fig. 20 Plot for voltage vs. current density and power density for 30 M.wt% NaAlg and 70 M.wt% NH_4ClO_4 and Nafion.™ 212

Comparison with Nafion.™ 212

Using a Nafion™ 212 membrane PEM fuel cell has been constructed under the similar condition used for NaAlg (30 NaAlg:70 NH_4ClO_4), and results are provided in Table 9. Nafion™ 212 membrane, the V_{oc} of 793 mV has been obtained (Fig. 17b). The voltage and corresponding current plotted as graph (Fig. 19).

Power density and current density have been calculated for the fuel cell constructed with the 30 M.wt% NaAlg: 70 M.wt% NH_4ClO_4 and Nafion™ 212 under similar condition. The results are shown in Fig. 20.

Conclusion

Solution casting technique has been used to develop a solid biopolymer electrolyte system based on sodium alginate (NaAlg) with a various NH_4ClO_4 concentrations. XRD reveal the amorphousness of the biopolymer electrolytes. The complex formation between the salt and the biopolymer is confirmed by the FTIR study. DSC studies have determined the glass transition temperature. The impedance study showed that the 30 M. wt% NaAlg:70 M.wt% NH_4ClO_4 has the highest ionic conductivity of 3.59×10^{-3} S cm^{-1}. The measurement of the transference number is done to confirm that the conduction occurs mainly by ions. The primary proton battery and PEM fuel cell have been constructed with highest conducting biopolymer electrolyte exhibits a V_{oc} of 1.76 V and 789 mV. It is clear from the results that the synthesized biopolymer electrolyte based on NaAlg and NH_4ClO_4 is more effective to be used with solid state electrochemical devices.

Author contributions Entire work has been done by N. Vanitha, and full manuscript has been written by N. Vanitha. The full manuscript has been corrected by C. Shanmugapriya. The concept of the work is given by S. Selvasekarapandian. FTIR study has been done by Muniraj Vignesh N. Linear sweep voltammetry study has been done by Aafrin Hazaana S. DSC analysis has been done by Meera Naachiyar R. Fuel cell construction work has been done by Kamatchi Devi S.

Data availability The datasets generated during and/or analyzed during the current study are not publicly available due to the manuscript is not yet published, but are available from the corresponding author on reasonable request.

Declarations

Ethics approval Not applicable.

Conflict of interest The authors declare no competing interests.

References

1. Kim JG, Son B, Mukherjee S, Schuppert N, Bates A, Kwon O, Choi MJ, Chung HY, Park S (2015) A review of lithium and non lithium based solid state batteries. J Power Sources 282:299–322
2. Khan NM, Ali NSM, Fuzlin AF, Samsudin AS (2020) Ionic conductiviy of alginate-NH_4Cl polymer electrolyte. Makara J Technol 24(3):5
3. Liu YH, Zhu LQ, Shi Yi, Wan Q (2014) Proton conducting sodium alginate electrolyte laterally coupled low- voltage oxide – based transistors. Appl Phys Lett 104(133504):1–4
4. Gao H, Lian K (2014) Proton –conducting polymer electrolytes and their applications in solid supercapacitors a review. J RSC Adv 4:33091–33113
5. Fuzlin AF, Saadiah MA, Yao Y, Nagao Y, Samsudin AS (2020) Enhancing proton conductivity of sodium alginate doped with glycolic acid in bio-based polymer electrolytes system. J Polym Res 207:1–16
6. Premalatha M, Mathavan T, Selvasekarapandian S, Monisha S, Pandi DV, Selvalakshmi S (2016) Investigations on proton conducting biopolymer membranes based on tamarind seed polysaccharide incorporated with ammonium thiocyanate. J Non-Cryst Solids 453:131–140
7. Draget KI, Skjak-Braek G, Christensen BE, Gaserod O, Smidsrod O (1996) Swelling and partial solubilization of alginic acid gel beads in acidic buffer. CarbohydratePolym 29:209–215
8. Yeom CK, Lee KH (1998) Characterization of sodium alginate membrane crosslinked with glutaraldehyde in pervaporation separation. J Appl Polym Sci 67:209–219
9. Salisu A, MohdMarsinSanagi AA, Naim WA, Ibrahim W, Karim KA (2015) Removal of lead ions from aqueous solutions using sodium alginate-graft-poly (methyl methacrylate) beads. J Desalination and Water Treatment 57:15353–15361
10. Oliveira Filho JG, Rodrigues JM, Valadares ACF, Almeida AB, Lima TM, Takeuchi KP (2019) Active food packaging: alginate films with cottonseed protein hydrolysates. Food Hydrocolloids 92:267–275
11 Akin Alper, NuranIsiklan, (2016) Microwave assisted synthesis and characterization of sodium alginate-graft-poly (N, N-dimethylacrylamide). Int J of Biol Macromol 82:530–540
12. Chen W, Feng Q, Zhang G, Yang Q, Zhang C (2017) The effect of sodium alginate on the flotation separation of scheelite from calcite and fluorite. Miner Eng 113:1–7
13. Bae SB, Nam HC, Park WH (2019) Electro spraying of environmentally sustainable alginate microbeads for cosmetic additives. Int J Biol Macromol 133:278–283
14. Sreekanth Reddy O, Subha MCS, Jithendra T, Madhavi C, Chowdoji Rao K (2020) Curcumin encapsulated dual cross linked sodium alginate/montmorillonite polymeric composite beads for controlled drug delivery. J Pharmaceutical Anal 20:31022–31024
15. Satheeshbabu BK, Mohamed I (2015) Synthesis and characterization of sodium alginate conjugate and study of effect of conjugation on drug release from matrix tablet. Indian J Pharm Sci 77:579–585
16. Reddy PRS, Rao KM, Rao KSVK (2014) Synthesis of alginate based silver nanocomposite hydrogels for biomedical applications. Macromol Res 22:832–842
17 Li J, He J, Huang Y (2017) Role of alginate in antibacterial finishing of textiles. Int J of Biol Macromol 94:466–473
18. Iwaki YO, Hernandezescalona M, Briones JR, Pawlicka A (2012) Sodium alginate based ionic conducting membranes. Mol Cryst Liq Cryst 554:221–231
19. Mohanapriya S, Bhat SD, Sahu AK, Manokaran A, Vijayakumar R, Pitchumani S, Sridhar P, Shukla AK (2010) Sodium alginate

based proton exchange membranes as electrolyte for DMFCs. Energy Environ Sci 3:1746–1756
20. Jansi R, Shenbagavalli S, Revathy MS, Deepalakshmi S, Indumathi P, Mohammed KA (2023) Structural and ionic transport in biopolymer electrolyte-based PVA:NaAlg with NH_4Cl for electrochemical applications. J.Materials science: Materials in Electronics 34:963
21. Diana MI, Lakshmi D, Christopher Selvin P, Selvasekarapandian S (2022) Substantial ion conduction in the biopolymer membrane: efficacy of NaI on sodium alginate matrix. J Materials letters 312:131652
22. Diana MI, Selvasekarapandian S, Christopher Selvin P, Vengadesh Krishna M (2022) A physicochemical elucidation of sodium perchlorate incorporated alginate biopolymer: toward all-solid-state sodium-ion battery. J Materials Science 57:8211–8224
23. Diana MI, Christopher Selvin P, Selvasekarapandian S, Vengadesh Krishna M (2021) Investigations on Na-ion conducting electrolyte based on sodium alginate biopolymer for all-solid-state sodium-ion batteries. J Solid State Electrochem 25:2009–2020
24. Tamilisai R, Palanisamy PN, Selvasekarapandian S, Maheshwari T (2021) Sodium alginate incorporated with magnesium nitrate as a novel solid biopolymer electrolyte for magnesiumion batteries. J Mater Sci: Mater Electron 32:22270–22285
25. Christopher Selvin P, Perumal P, Selvasekarapandian S, Monisha S, Boopathi G, Leena Chandra MV (2018) Study of proton-conducting polymer electrolyte based on K-carrageenan and NH_4SCN for electrochemical devices. Ionics 24:3535–3542
26. Vanitha N, Shanmugapriya C, Selvasekarapandian S, Naachiyar RM, Krishna MV, Aafrin S, Nandhini K (2022) Effect of graphene quantum dot on sodium alginate with ammonium formate (NH_4HCO_2) biopolymer electrolytes for the application of electrochemical devices. Ionics 28:2731–2749
27. Selvalakshmi S, Mathavan T, Selvasekarapandian S, Premalatha M (2018) A study of electrochemical devices based on Agar-Agar-NH_4I biopolymer electrolytes. AIP conference proceedings 1942(1):140019
28. Selvalakshmi S, Mathavan T, Selvasekarapandian S, Premalatha M (2018) Effect of ethylene carbonate plasticizer on agar-agar: NH_4Br-based solid polymer electrolytes. Ionics 24:2209–2217
29. Aziz SB, Brza MA, Saed SR, Hamsan MH, Kadir MFZ (2020) Ion association as a main shortcoming in polymer blend electrolytes based on GS:PS incorporated with various amounts of ammonium tetrafluoroborate. J Mater Res Technol 9:5410–5421
30. Aziz SB, Nofal MM, Rebar T, Abdulwahid KMFZ, Hadi JM, Hessien MM, Kareem WO, Dannoun EMA, SaeedImpedance SR (2021) FTIR and transport properties of plasticized proton conducting biopolymer electrolyte based on chitosan for electrochemical device application. J Results in Physics 29:104770
31. Sohaimy MIH, Natural IMIN (2020) Inspired carboxymethyl cellulose (CMC) doped with ammonium carbonate (AC) as biopolymer electrolyte. J Polymers 12:2487
32. Sohaimy MIH, Isa MIN (2022) Proton-conducting biopolymer electrolytes based on carboxymethyl cellulose doped with ammonium formate. J Polymers 14:3019
33. Ramlli MA, Isa MINM, Kamarudin KH (2022) 2-Hydroxyethyl cellulose-ammonium thiocyanate solid biopolymer electrolytes: ionic conductivity and dielectric studies. J Sustain Sci Management 17:121–132
34. Muthukrishnan M, Shanthi C, Selvasekarapandian S, Shanthi G, Sampathkumar L, Maheshwari T (2021) Impact of ammonium formate (AF) and ethylene carbonate (EC) on the structural, electrical, transport and electrochemical properties of pectin-based biopolymer membranes. Ionics 27:3443–3459
35. Muthukrishnan M, Shanthi C, Selvasekarapandian S, Premkumar R (2023) Biodegradable flexible proton conducting solid biopolymer membranes based on pectin and ammonium salt for electrochemical applications. Int J Hydrogen Energy 48:5387–5401
36. Maheshwari T, Tamilarasan K, Selvasekarapandian S, Chitra R, Kiruthika S (2021) Investigation of blend biopolymer electrolytes based on dextran-PVA with ammonium thiocyanate. J Solid State Electrochem 25:755–765
37. Meera Naachiyar R, Ragam M, Selvasekarapandian S, Aristatil AafrinHazaana, Muniraj Vignesh N, Vengadesh Krishna M (2022) Fabrication of rechargeable proton battery and PEM fuel cell using biopolymer gellan gum incorporated with NH_4HCO_2 solid electrolyte. J Polym Res 29:337
38. Vanitha N, Shanmugapriya C, Selvasekarapandian S, VengadeshKrishna NK (2022) Investigation of N-S-based graphene quantum dot on sodium alginate with ammonium thiocyanate (NH4SCN) biopolymer electrolyte for the application of electrochemical devices. J Materials Sci: Materials Electronics 33:14847–14867
39. Hajifathaliha F, Mahboubi A, Nematollahi L, Mohit E, Bolourchian N (2018) Comparison of different cationic polymers efficacy in fabrication of alginate multilayer microcapsules. Asian J Pharmaceutical Sciences 15:95–103
40. Rasali NMJ, Samsudin AS (2018) Characterization on ionic conductivity of solid bio-polymer electrolytes system based alginate doped ammonium nitrate via impedance spectroscopy. AIP conference proceeding 2020:1–8
41. Hodge RM, Edward GH, Simon GP (1996) Water absorption and states of water in semicrystalline poly(vinyl alcohol) films. Polymer 37:1371–1376
42. Sridevi D, Rajendran KV (2009) Synthesis and optical characteristics of ZnO nanocrystals. Bull Master Sci 32(2):165–168
43. Vij A, Chawla AK, Kumar R, Lochab SP, Chandra R, Singh N (2010) Effect of 120 MeV $Ag9^+$ ion beam irradiation on the structure and photoluminescence of SrS: Ce nanostructures. Phys B 405(11):2573–2576
44. Mangalam R, Thamilselvan M, Selvasekarapandian S, Jayakumar S, Manjuladevi R (2017) Magnesium ion conducting polyvinyl alcohol–polyvinyl pyrrolidone-based blend polymer electrolyte. Ionics 23:1771–1781
45. Zhi J, Tian-Fang W, Shu-Fen L, Feng-Qi Z, Zi-Ru L, Cui-Mei Y, Yang L, Shang-Wen L, Gang-Zhui Z (2006) Thermal behavior of ammonium perchlorate and metal powders of different grades. J Therm Anal Calorim 85:315–320
46. Helmiyati AM (2017) Characterization and properties of Sodium alginate from brown algae used as an ecofriendly superabsorbent. IOP Conf Ser Mater Sci Eng 188:12019
47. Fuzlin AF, Bakri NA, Sahraoui B, Samsudin AS (2020) Study on the effect of lithium nitrate in ionic conduction properties based alginate biopolymer electrolytes. Mater Res Express 7:015902
48. Aprilliza M (2017) Characterization and properties of sodium alginate from brown algae used as an ecofriendly superabsorbent. IOP Conf Ser Mater Sci Eng 188:12019
49. Kanti P, Srigowri K, Madhuri J, Smitha B, Sridhar S (2004) Dehydration of ethanol through blend membranes of chitosan and sodium alginate by pervaporation. Sep Puri Technol 40:259–266
50. Moniha V, Marimuthu A, Selvasekarapandian S, Sundaresan B, Hemalatha R (2019) Development and characterization of biopolymer electrolyte iota-carrageenan with ammonium salt for electrochemical application. Mater Today Proc 8:449–455
51. Moniha V, Alagar M, Selvasekarapandian S, Sundaresan B, Hemalatha R, Boopathi G (2018) Synthesis and characterization of bio-polymer electrolyte based on iota-carrageenan with ammonium thiocyanate and its applications. J Solid State Electrochem 22:3209–3223
52. Maheshwari T, Tamilarasan K, Selvasekarapandian S, Chitra R, Muthukrishnan M (2021) Synthesis and characterization of dextran, poly (vinyl alcohol) blend biopolymer electrolytes with

NH_4NO_3, for electrochemical applications. Int J Green Energy 19:314–330
53. Fuzlin AF, Samsudin AS (2021) Studies on favorable ionic conduction and structural properties of biopolymer electrolytes system-based alginate. J Polym Bull 78:2155–2175
54. Boukamp BA (1986) A nonlinear least square fit procedure for analysis of impedance data of electrochemical systems. Solid State Ionics 20:31–44
55. Karthikeyan S, Sikkanthar S, Selvasekarapandian S, Arunkumar D, Nithya H, Iwa Y, Kawamura J (2016) Structural, electrical and electrochemical properties of polyacrylonitrile-ammonium hexaflurophosphate polymer electrolyte system. J Polym Res 23:51
56. Rasali NMJ, Nagao Y, Samsudin AS (2019) Enhancement on amorphous phase in solid biopolymer electrolyte based alginate doped NH_4NO_3. Journal of Ionics 25:641–654
57. Moniha V, Alagar M, Selvasekarapandian S, Sundaresan B, Boopathi G (2018) Conductive bio-polymer electrolyte iota-carrageenan with ammonium nitrate for application in electrochemical devices. J Non-Cryst Solids 481:424–434
58. Monisha S, Mathavan T, Selvasekarapandian S, Milton Franklin Benial A, Aristatil G, Mani N, Premalatha M, Vinoth Pandi D (2017) Investigation of bio polymer electrolyte based on cellulose acetate-ammonium nitrate for potential use in electrochemical devices. CarbohydrPolym 157:38–47
59. Hashmi SA, Chandra S (1995) Experimental investigations on a sodium- ion- conducting polymer electrolyte based on poly(ethylene oxide) complexed with NaPF6. Mater Sci Eng B 34:18–26
60. Wagner JB, Wagner CJ (1957) Electrical conductivity measurements on curprous halides. J Chem Phys 26:1597–1601
61. Mahalakshmi M, Selvanayagam S, Selasekarapandian S, Monisha V (2019) Characterization of biopolymer electrolytes based on cellulose acetate with magnesium perchlorate ($Mg(ClO_4)_2$) for energy storage devices. J Sci Adv Materials Devices 4:276–284
62. Selvalakshmi S, Mathavan T, Selvasekarapandian S, Premalatha M (2019) Characterization of biodegradable solid polymer electrolyte system based on agar-NH_4Br and its comparison with NH_4I. J Solid State Electrochem 23:1727–1737
63. Pandey K, Lakshmi N, Chandra S (1998) A rechargeable solid state proton battery with an intercalating cathode and an anode containing a hydrogen storage-material. J Power Sources 76(1):116–123
64. Meera Naachiyar R, Ragam M, Selvasekarapandian S, Vengadesh Krishna M, Buvaneshwari P (2021) Development of biopolymer electrolyte membrane using gellan gum biopolymer incorporated with NH_4SCN for electro-chemical application. J Ionics 27:3415–3429
65. Tang Y, Yuan W, Pan M, Wan Z (2010) Feasibility study of porous copper fiber sintered felt: a novel porous flow field in proton exchange membrane fuel cells. Int J Hydrogen Energy 35:9661–9677